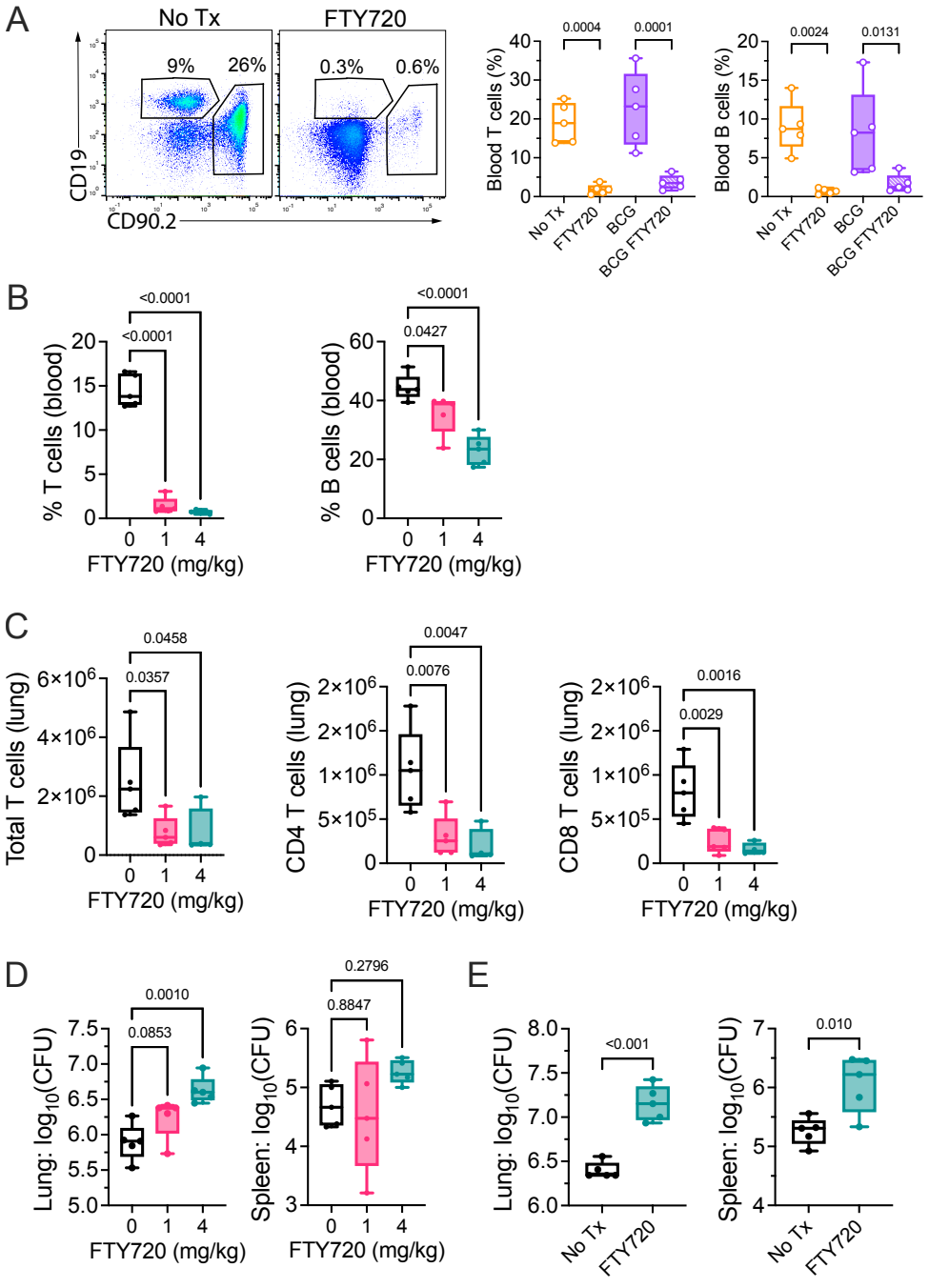
A
No Tx
FTY720
9%
26%
0.3%
0.6%
CD19
CD90.2
Blood T cells (%)
0.0004
0.0001
Blood B cells (%)
0.0024
0.0131
No Tx
FTY720
BCG
BCG FTY720
B
% T cells (blood)
<0.0001
<0.0001
% B cells (blood)
<0.0001
0.0427
FTY720 (mg/kg)
C
Total T cells (lung)
0.0458
0.0357
CD4 T cells (lung)
0.0047
0.0076
CD8 T cells (lung)
0.0016
0.0029
FTY720 (mg/kg)
D
Lung: log10(CFU)
0.0010
0.0853
Spleen: log10(CFU)
0.2796
0.8847
FTY720 (mg/kg)
E
Lung: log10(CFU)
<0.001
Spleen: log10(CFU)
0.010
No Tx
FTY720

Figure S1

Figure S1. Optimization of FTY720 use in the murine TB model (pertains to Fig.3)

A. Treatment of B6 mice with FTY720 after Mtb infection led to a reduction in the percentage of T cells (left) and B cells (right) among all live cells in peripheral blood as determined by flow cytometry.

B. Treatment with FTY720 led to significant reductions in the frequency of both T (left) and B (right) cells in the blood of B6 mice after Mtb infection.

C. Treatment with FTY720 led to significant reductions in the number of total T cells (left) including CD4 (middle) and CD8 (right) T cells in the lungs of Mtb infected B6 mice.

D. The bacterial burden in the lungs (left) or spleens (right) of infected B6 mice was increased when treated with 4 mg/kg of FTY720, but not 1 mg/kg of FTY720, as determined four wpi. FTY720 did not have a significant effect on Mtb control in the spleens of treated mice. One-way ANOVA with Dunnett's multiple comparisons test.

E. CFU in the lung (left) and spleen (right) of B6 mice at four wpi. This experiment performed in parallel with the one with CC042 mice depicted in Figure 3.

n=4-5 mice/group. One-way ANOVA with Dunnett's multiple comparisons test (A-D) or t-test (E). Data is representative of one (A-D) or two (E) individual experiments. Box plots indicate median (middle line), 25th, 75th percentile (box) and minimum and maximum (whiskers).

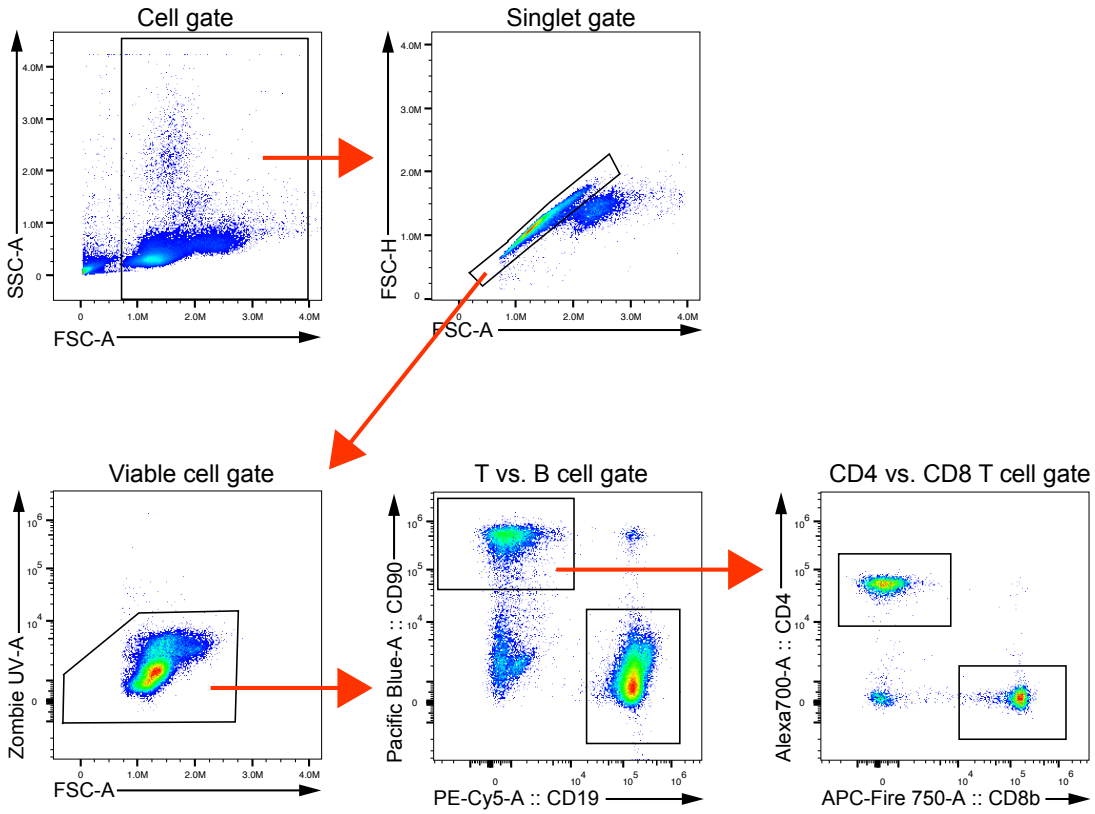

Figure S2. Gating Scheme for Identifying B & T cells in Peripheral Blood

Gating strategy for identifying B and T cells in the peripheral blood. In brief, doublets were excluded and then a viability dye was used to exclude dead cells. B cells were identified by expression of CD19 while T cells were identified by expression of CD90 or CD3. Then, CD4 and CD8α or CD8β was used to specifically identify CD4 T and CD8 T Cells.

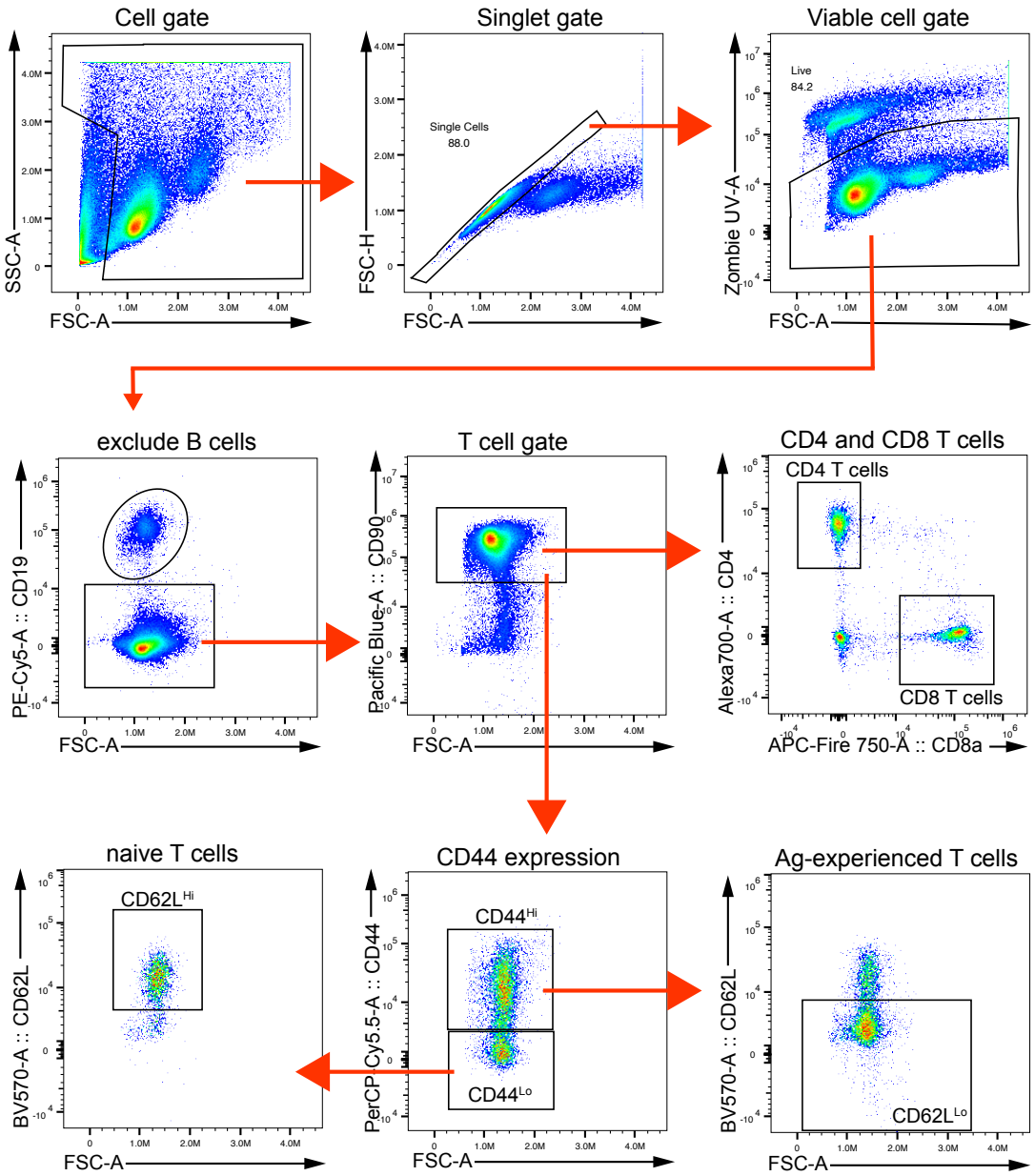

Figure S3. Gating Scheme for Identifying T cells in Lung

Gating strategy for identifying T cell population in the lung. In brief, doublets were excluded and then a viability dye was used to exclude dead cells. B cells were then excluded by expression of CD19, while T cells were identified by expression of CD90. T cells were then subclassified by CD4 or CD8 by their expression of CD4 or CD8α or CD8β, respectively. Naïve T cells were identified by the expression of CD62L and lack of CD44 expression. Antigen-experienced T cells were identified by expression of CD44 and lack of expression of CD62L.

A

Specificity	Primary antibody (in vivo depleting)	Secondary antibody (in vitro staining)	Cross-blocking?
CD4	GK1.5	GK1.5	yes
		RM4-4	no
		RM4-5	no
CD8a	2.4.3	53-6.7	no
		YTS156.7.7	no
CD20	MB20-11	6D5	no

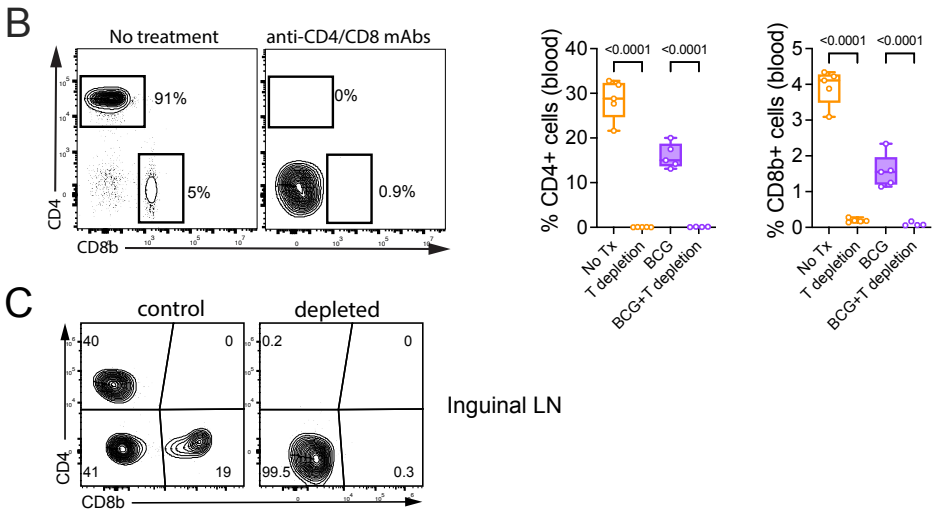

Figure S4

Figure S4. T cell depletion strategies (pertains to Fig.4)

A. Evaluation of antibody cross-blocking potential in CC042 mice. The anti-CD4 mAb GK1.5 that is used to deplete CD4 T cells in vivo blocked the binding of labeled GK1.5, but not of alternate anti-CD4 mAbs RM4-4 or RM4-5. The anti-CD8α mAb used in vivo (clone 2.4.3) does not block binding of alternate anti-CD8α clone 53-6.7 or anti-CD8β clone YTS156.7.7. Therefore, the efficiency of CD4 and CD8 T cell depletion in vivo by GK1.5 and 2.4.3 was quantified using anti-CD4 mAbs RM4-4 or RM4-5 and anti-CD8α mAb 53-6.7 or CD8β YTS156.7.7 in all T cell depletion experiments. Similarly, the anti-CD20 mAb MB20-11, used to deplete B cell in vivo, did not inhibit the binding of anti-CD19 mAb clone 6D5 to B cells.

B. Representative flow plot of CD4 and CD8β expression of $CD90^+$ T cells in the blood at four wpi of a representative untreated CC042 mouse and one treated with anti-CD4 and anti-CD8α mAbs (left). Frequency of $CD90^+$ CD4 and CD8β T cells in blood at the end of the depletion period before Mtb infection of CC042 mice (Right).

C. Representative flow plot demonstrating CD4 and CD8 T cell depletion in the inguinal LN from BCG-vaccinated CC042 mice after treatment with anti-CD4 and anti-CD8 mAbs as described in the *Methods.*

D. Depletion of CD4 and CD8 T cells from the lungs (top) and spleens (bottom) of CC042 mice. CC042 mice were vaccinated with BCG and treated with anti-CD4 and anti-CD8 mAbs as described in the *Methods*. Cells were stained with markers for CD4 and CD8 T cells, and NK (NKp46) cells.

One-way ANOVA with Šídák's multiple comparisons test (B) Or Mann-Whitney t-test (D). Data are representative or two (D) or three (B, C) independent experiments with similar results. Each point represents an individual subject, n=5 mice per group. Box plots indicate median (middle line), 25th, 75th percentile (box) and minimum and maximum (whiskers).

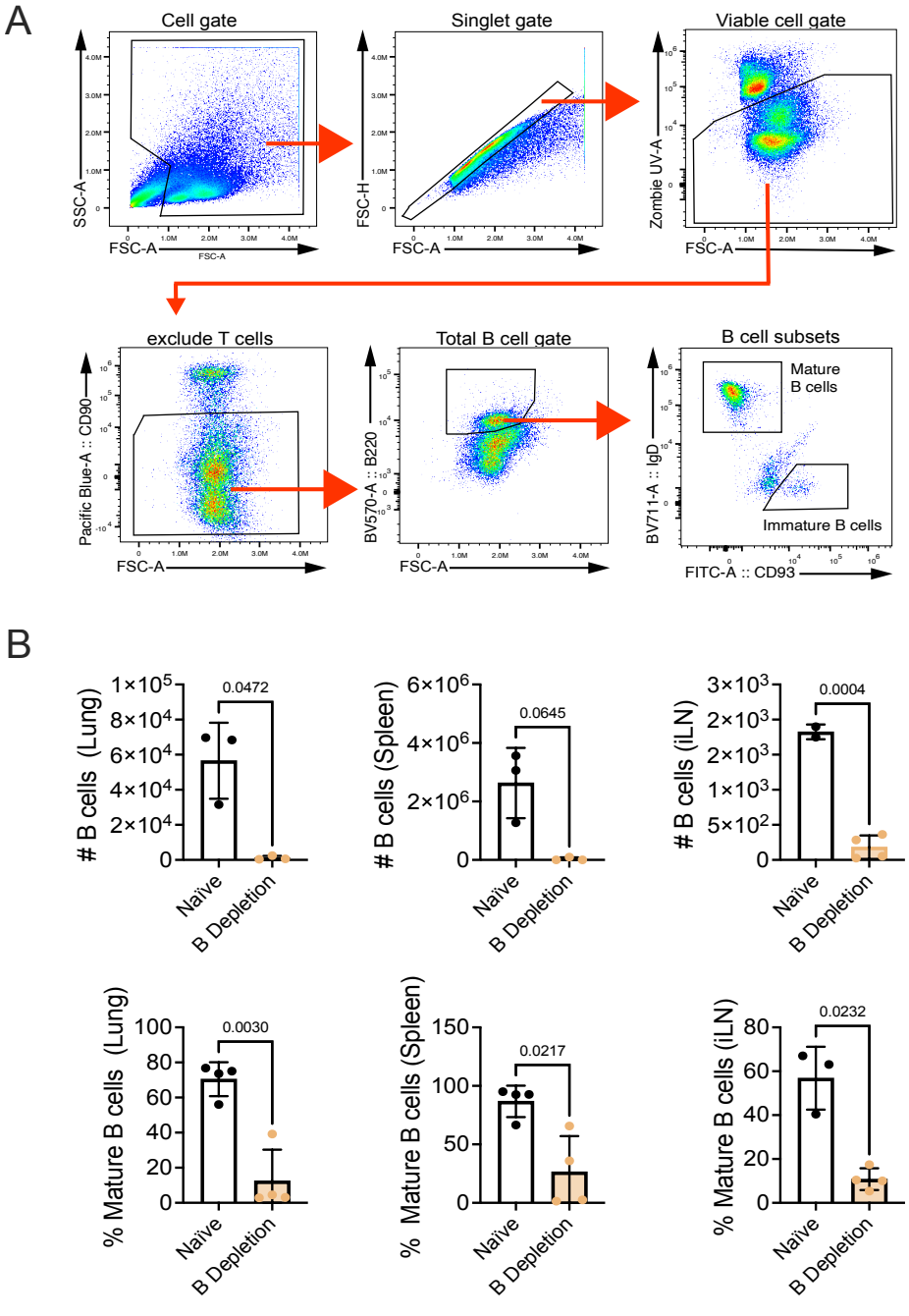

Figure S5

63
64

Figure S5. B cell depletion strategies (pertains to Fig.5)

A. Gating strategy for identifying B cell populations in the lung, lymph node and spleen. In brief, doublets were excluded and then a viability dye was used to exclude dead cells. T cells were excluded by the expression of CD90. Total B cells were identified by the expression of B220. B cells were then further classified as mature or immature. Mature B cells were identified by expression of IgD and lack of CD93 expression, while immature B cells were identified by expression of CD93 and lack of IgD expression.

B. Number of total B cells (top row) and frequency of mature ($B220^{+}IgD^{+}CD93^{-}$) B cells as a percentage of total B cells (bottom row) in the lung (left), spleen (middle) and iLN (right), two weeks after a single administration of anti-CD20 mAb to naïve CC042 mice. Data represents two experiments. Each point is an individual subject, n=3-4 mice per group. Unpaired t-test. Bars, mean. Line, SD.

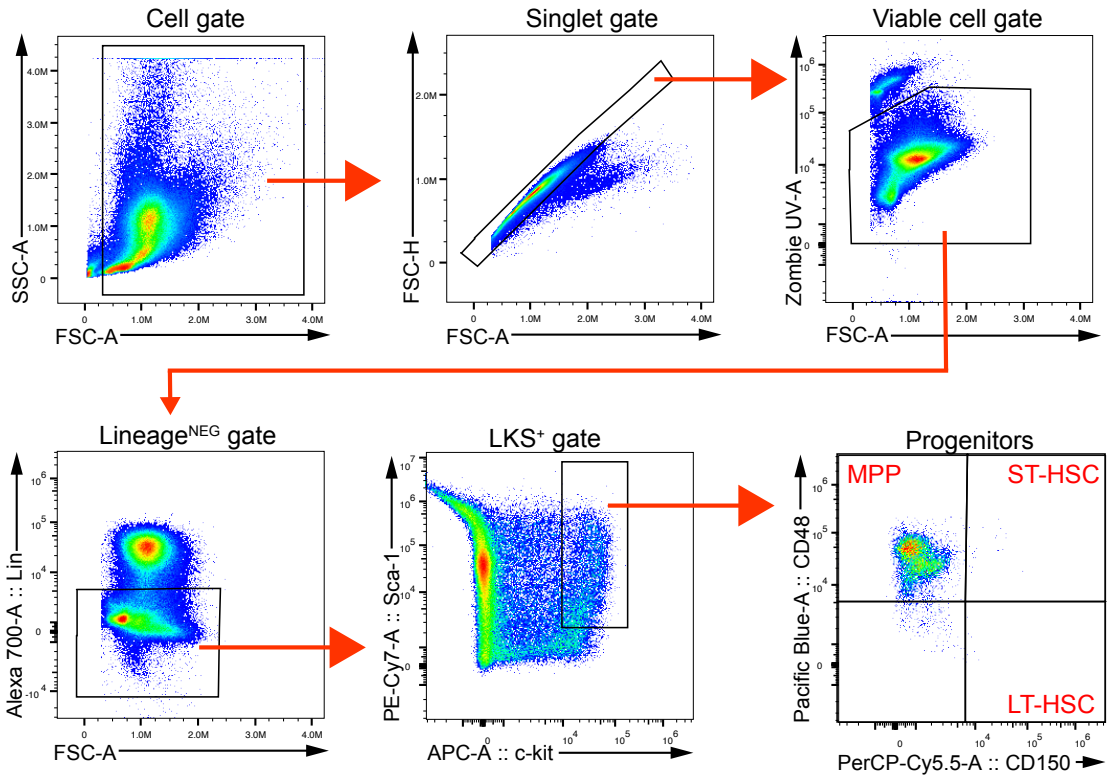

77

78 **Figure S6. Gating Scheme for Identifying LKS+ Cells in Bone Marrow**

79 Gating strategy for identifying LKS+ hematopoietic stem cells in the bone marrow. Doublets were
80 excluded and then a viability dye was used to exclude dead cells. LKS+ cells were then identified
81 by the lack of expression of a lineage marker and co-expression of Sca-1 and c-kit. LKS+ cells
82 were then further sub-divided into MPP, ST-HSC and LT-HSC by differential expression of CD48
83 and CD150.

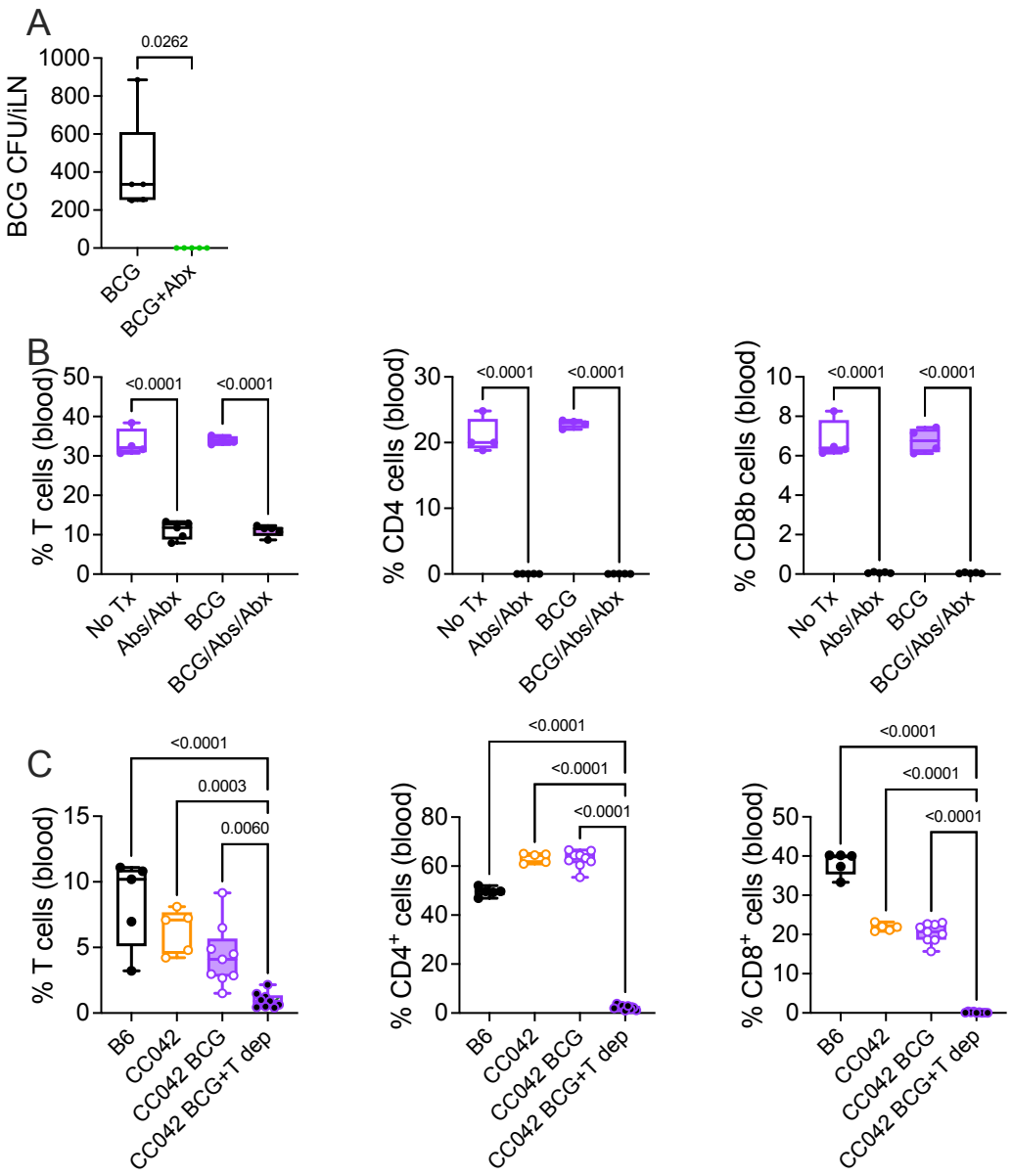

Figure S7

84

85

Figure S7. Efficacy of antibiotic treatment and combined T cell depletion strategy (pertains to Fig.7)

A. BCG in LNs is cleared by antibiotics. One of two independent experiments. Each dot represents an individual mouse, n=5 mice per group. Paired t-test. The limit of detection = 5 CFU.

B. Frequency of total $CD90^+$ T cells (right), CD4 (middle) or CD8 (left) T cells in peripheral blood as a percentage of total live cells. Groups are untreated CC042 mice (No Tx), unvaccinated CC042 mice treated with anti-CD4 + anti-CD8α mAbs and antibiotics (Abs/Abx), BCG-vaccinated CC042 mice (BCG) or BCG-vaccinated CC042 mice treated with anti-CD4 + anti-CD8α mAbs and antibiotics (BCG/Abs/Abx).

C. Frequency of total $CD90^+$ T cells (right), CD4 (middle) or CD8 (left) T cells in peripheral blood as a percentage of total live cells. Groups are unvaccinated B6 mice (B6), unvaccinated CC042 mice (CC042), BCG-vaccinated CC042 mice (BCG) or BCG-vaccinated CC042 mice treated with anti-CD4 + anti-CD8α mAbs (CC042 BCG+T Dep).

B, C. Data is representative of 2 experiments with similar results. Each point is an individual subject, n=4-9. Bars, mean. One-way ANOVA with Šídák's multiple comparisons test. Box plots indicate median (middle line), 25th, 75th percentile (box) and minimum and maximum (whiskers).

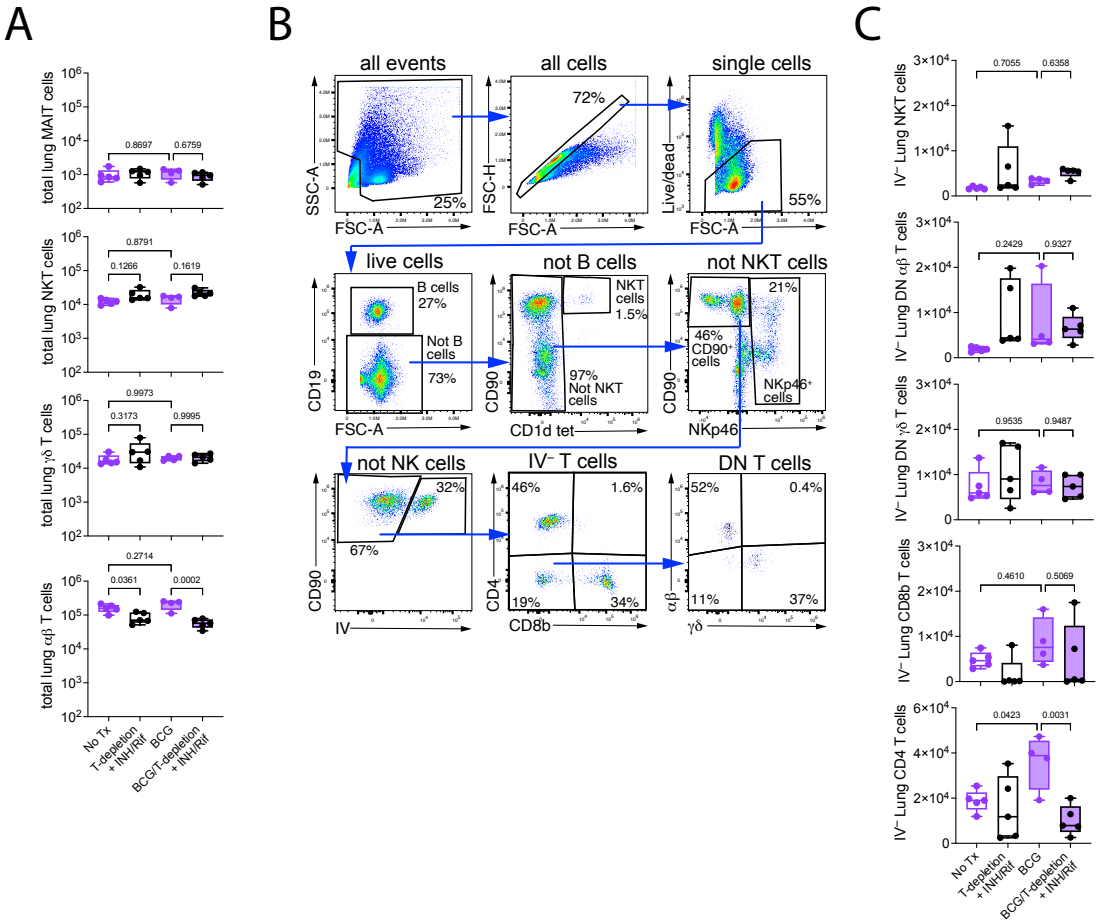
A
B
C
total lung MAIT cells
total lung NKT cells
total lung γδ T cells
total lung αβ T cells
0.8697
0.6759
0.8791
0.1266
0.1619
0.9973
0.3173
0.9995
0.2714
0.0361
0.0002
No Tx
T-depletion + INH/Rif
BCG
BCG/T-depletion + INH/Rif
all events
all cells
single cells
SSC-A
FSC-A
25%
FSC-H
72%
Live/dead
55%
live cells
not B cells
not NKT cells
B cells 27%
Not B cells 73%
CD19
NKT cells 1.5%
97% Not NKT cells
CD90
CD1d tet
21%
46% CD90+ cells
NKp46+ cells
NKp46
not NK cells
IV⁻ T cells
DN T cells
32%
67%
IV
46%
1.6%
19%
34%
CD4
CD8b
52%
0.4%
11%
37%
αβ
γδ
IV⁻ Lung NKT cells
IV⁻ Lung DN αβ T cells
IV⁻ Lung DN γδ T cells
IV⁻ Lung CD8b T cells
IV⁻ Lung CD4 T cells
0.7055
0.6358
0.2429
0.9327
0.9535
0.9487
0.4610
0.5069
0.0423
0.0031

102

103

Figure S8. T cells in the lung parenchyma after Mtb infection (pertains to Fig.7)

A. Different types of T cells were enumerated in the lungs of mice treated as shown in Fig.7D-E, 4 weeks after Mtb challenge. MAIT and NKT cells identified using tetramers.

B. Gating strategy to measure different T cell classes and their location in the lung. Intravascular cells were identified by injecting fluorochrome labelled antibodies intravenously, 3 minutes prior to euthanasia.

C. Number of lung parenchyma (i.e., IV^-) T cell subsets in unvaccinated and BCG vaccinated CC042 mice after treatment (see Fig.7D), measured four weeks after Mtb infection.

Representative result from one of two independent experiments using untreated CC042 mice (No Tx), unvaccinated CC042 mice treated with anti-CD4 + anti-CD8α mAbs and antibiotics (T-depletion + INH/Rif), BCG-vaccinated CC042 mice (BCG) or BCG-vaccinated CC042 mice treated with anti-CD4 + anti-CD8α mAbs and antibiotics (T-depletion + INH/Rif). Each dot represents an individual mouse, n=4-5 mice per group. One-way ANOVA with Šídák's multiple comparisons test. Box plots indicate median (middle line), 25th, 75th percentile (box) and minimum and maximum (whiskers).

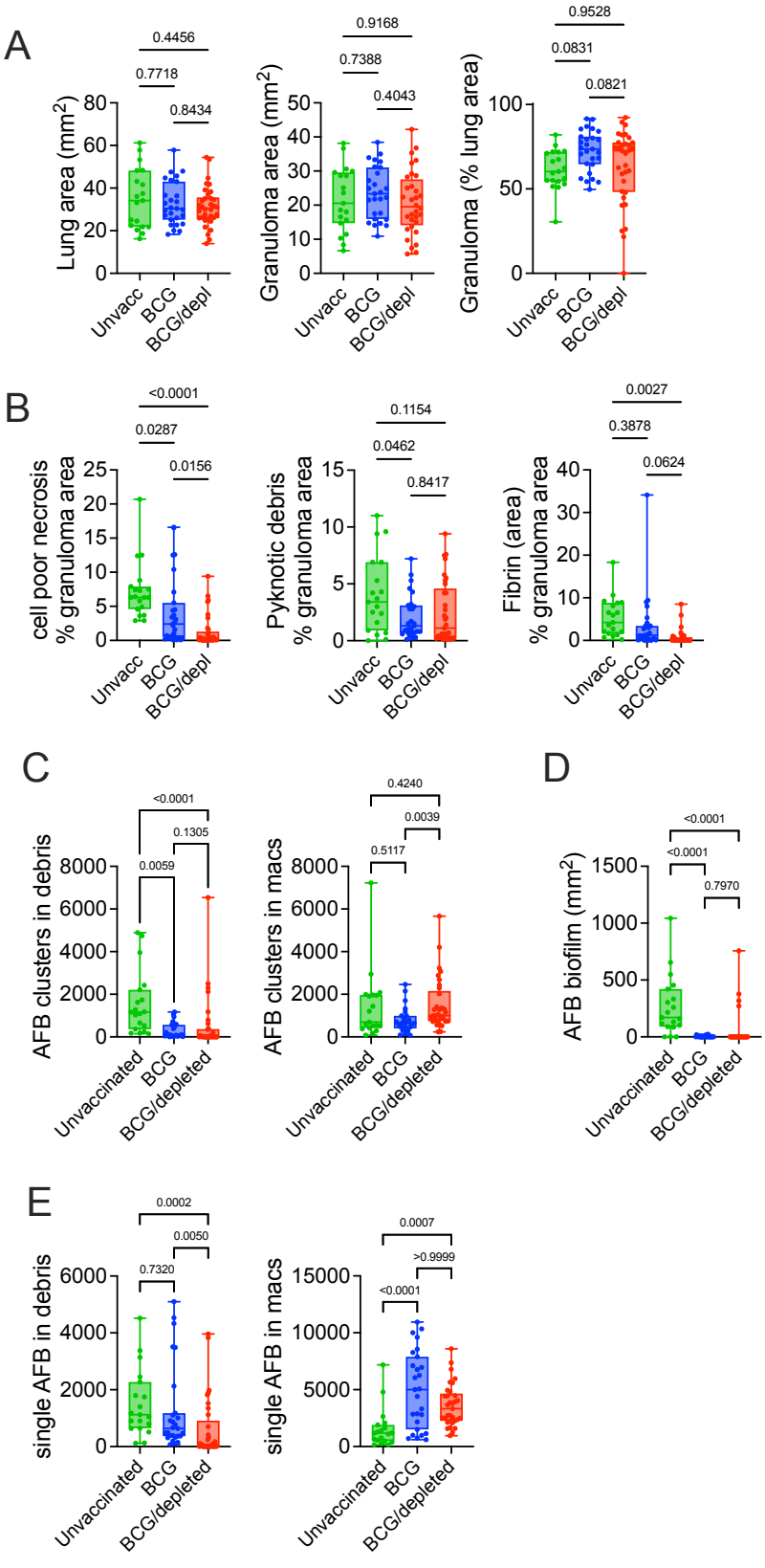
A
Lung area (mm2)
0.4456
0.7718
0.8434
Granuloma area (mm2)
0.9168
0.7388
0.4043
Granuloma (% lung area)
0.9528
0.0831
0.0821
Unvacc
BCG
BCG/depl
B
cell poor necrosis % granuloma area
<0.0001
0.0287
0.0156
Pyknotic debris % granuloma area
0.1154
0.0462
0.8417
Fibrin (area) % granuloma area
0.0027
0.3878
0.0624
C
AFB clusters in debris
<0.0001
0.1305
0.0059
AFB clusters in macs
0.4240
0.0039
0.5117
Unvaccinated
BCG
BCG/depleted
D
AFB biofilm (mm2)
<0.0001
<0.0001
0.7970
E
single AFB in debris
0.0002
0.0050
0.7320
single AFB in macs
0.0007
>0.9999
<0.0001

119

120

Figure S9. Histological analysis (pertains to Fig.8)

A-D. Automated image analysis of histopathological tissue**.** Three to five lung lobes were analyzed per mouse for a total of 19 (unvaccinated), 27 (BCG), and 34 (BCG+T depletion). **A**. The total area of each scanned lung (left), the total area occupied by lesional tissue (i.e., granulomas, center), and the percentage of the lung occupied by granulomas (right). **B**. Analysis of parameters related to tissue death and destruction including the percentage of lung occupied by cell poor necrosis (left), the percentage of pyknotic debris (middle), and the amount of fibrin (right). **C**. Measurement of parameters relating to the bacterial burden including, from left to right, the number of AFB clusters in debris or in macrophages. the number of single Mtb in debris or macrophages. **D**. The absolute area of AFB biofilm. **E**. The number of single Mtb in debris (left) or macrophages (right).

A-E. Comparisons between different groups were analyzed using a non-parametric one-way Anova (Kruskal-Wallis). Box plots indicate median (middle line), 25th, 75th percentile (box) and minimum and maximum (whiskers).